Astrophys Space Sci (2019) 364:211
https://doi.org/10.1007/s10509-019-3702-1

ORIGINAL ARTICLE

Seasonal variations of the electrostatic potential near auroral low latitudes

Rima Mebrek[1] · **Mourad Djebli**[1] · **Rachid Fermous**[2]

Received: 24 May 2019 / Accepted: 16 November 2019 / Published online: 25 November 2019

Abstract Based on the plasma expansion model, the mapping of ionospheric electrostatic potential (field) is derived at the first moments of sunrise and for different seasons, near auroral low latitude regions. For that purpose we considered an ionospheric altitude where one ion species is dominant which is O^+ (at ~ 400 km). Fluid equations are transformed into a simplified form by using quasi-neutrality assumption along with a self-similar approach. The qualitative variations of the electrostatic potential during different seasons show that the plasma dynamics depends on the solar activities, included through heavy species collision terms as well as the universal time. The negative electrostatic potential is established at the earlier stages during hotter seasons, while important drops are seen in the cold season.

Keywords Ionospheres · Expansion · Ionization

1 Introduction

The ionospheric potential is a simple scalar quantity that can be probed easily to give clues on temperature. The latter is connected to potential generators particularly in the equatorial, tropical and mid-latitudes regions through an independent parameter that makes possible comparison with measurements both on short and long terms (Markson and Price 1999). This potential is subject to changes due to lightning, sprites (Rycroft and Odzimek 2011) and probably to the penetration of an electrostatic field from the lithosphere into the higher ionosphere region. By using numerical techniques, Park et al. assumed an arbitrary potential distribution to calculate the electric field at mid-altitude, showing that the ionospheric electric fields map down to low altitudes very efficiently (Park 1976). Thus, the electric field plays also an important role such as that of a precursor of earthquakes by measuring penetration of an electric field produced at the Earth's surface to the ionosphere. Many satellite measurements reported fluctuations in ionospheric electron and ion densities prior to large earthquakes such as the one occurred near the south coast of Honshu, Japan. A fluctuation in the electron density, that inherently affects the plasma potential, was observed before the main earthquakes above the epicenter. It is suggested that the horizontal electric field at the lower boundary of the ionosphere have been strengthened by the seismic activity giving rise to the observed ionospheric anomalies (Ryu et al. 2014). By analyzing four huge earthquakes Fan et al. found that the ionospheric electric field increased abnormally before and after the earthquakes. The observation of the ionospheric electric field makes possible the detection of the low-frequency electromagnetic radiation during the imminent stages before earthquakes (Fan et al. 2015). It is also found that proton and ion density variations in ionosphere are observed before strong earthquake. These variations are significantly detected at night. The electric field is becoming stronger as a result of emerged submicron aerosols due to plate movements, by which ionosphere gets ionized (Hazra and Islam 2015). An other key factor that disturb the ionospheric plasma density may be the interaction of ion accumulation and upward movement from gas-water release at surface (Zhang et al. 2019). Thus, the natural ionospheric electric field has generated considerable interest in term of possible pre-seismic effects, significant changes have been reported in the electrical signals few days

✉ M. Djebli
mdjebli@usthb.dz

[1] Faculty of Physics, Theoretical Physics Laboratory, USTHB, B.P. 32 Bab-Ezzouar, 16079 Algiers, Algeria

[2] Faculté des Sciences et de la Technologie, Universite Djilali Bounaama Route de Theniet-el-Had, 44225 Khemis Miliana, Algeria

before a strong earthquakes. However, the penetration of the electric field from the Earth's surface to the ionosphere is too weak to be detected by satellite measurements on the background of usual ionospheric fields (Denisenko 2015). In addition, the main difficulty is to depict natural changes in the ionospheric electric filed since the measurements are inherently affected by the generated electric filed due to the motion of the satellite used to make measurements (Makhlouf and Djebli 2019). Therefore, it is necessarily to study other physical processes to understand disturbances associated to ionospheric electrostatic field.

Different models have been proposed to understand how the electrostatic field is generated in the ionosphere's layers. Stening (1973) considered an equivalent circuit method to calculate the current flow and then obtained the conductivity which depends on densities. Thus, variations in the ionospheric electrostatic field obtained by this model showed a good agreement with observed electrostatic field at certain regions. By using the plasma quasi-neutrality principle it was found that the presence of different charged particle populations in the ionosphere leads to the formation of a potential difference of up to several kilovolts for which electron precipitation is characterized by the corresponding electric field (Chiu and Schulz 1978).

In most ionospheres photoionization is the main source to produce electron-ion pairs. In the Earth's ionosphere, according to the model of neutral upper atmosphere, O^+ ions are produced by photoionization while H^+ ions result from charge transfer (Chang 1987). The maximum ionization by EUV (Extreme ultraviolet, 800–126 Å) radiation occurs at altitude $\sim$ 250–300 km in the F-region, where a dense layer of O^+ gets split into two distinct layers F_1 and F_2 (Haider et al. 2009). Moreover, numerical simulation shows that a solar flux variation induced plasma drift which affects the equatorial F-region (Watanabe et al. 1995).

Expansion is one of the major physical processes occurring in the atmosphere in which F-region is involved. It results from the changes arising from solar radiations heating during daytime and contraction due to cooling at night. The particles vertical distribution is modified by thermal transports (Rishbeth 1968). By using computer simulation Singh and Schunk studied an expanding plasma relevant to polar wind. The evolution of the expanding plasma was found to depend on the rates of minority species of such a plasma mix (Singh and Schunk 1982). Moreover, the expansion of space plasma involves interesting processes such as instabilities, discontinuities and energetic ions responsible for high-latitude ionosphere energization (Samir et al. 1983). In the upper F-region a hydrodynamical model has been used to study the early-time cloud plasma expansion showing that the electric field associated with the density gradient creates a hole in the ionosphere (Schunk and Szuszczewicz 1991).

The aim of the present work is to use the plasma expansion model to describe variations of the electrostatic potential that occur when the plasma of the Earth's ionosphere expands during the first moments of sunrise. In this study we include realistic simulation conditions, and we also consider the effect of energy transfer between different species constituting the ionospheric plasma. To address this problem and to solve the transport equations governing this phenomenon (Rishbeth and Garriott 1969), the self-similar approach is applied (Gurevich et al. 1966). The obtained solution makes possible the qualitative description of electric potential (field) seasonal variations.

2 Ionospheric plasma expansion model

In the ionosphere the electron density is subject to variations associated to solar activity. Thus, energetic particles precipitate and transfer their energy to the plasma which expands. Changes in O^+ density have been recorded in both E and F regions of the Earth's ionosphere. For the latter the effects are very important on the ground- and space-based technology systems (Buonsanto 1999). It is well known that in the F_2 region of the terrestrial ionosphere, the plasma is mainly produced by photoionization of neutral atoms and molecules constituting the atmosphere. The O^+ ions are being the dominant species in this region, where the peak is observed near $\sim$ 300 km. For this we consider three primary chemical processes (Rishbeth and Garriott 1969; Nagy et al. 2009)

$$O + h\nu \xrightarrow{p_r^{O^+}} O^+ + e \tag{1}$$

$$O_2 + h\nu \xrightarrow{p_r^{O_2^+}} O_2^+ + e \tag{2}$$

$$N_2 + h\nu \xrightarrow{p_r^{N_2^+}} N_2^+ + e \tag{3}$$

The molecular recombination of O^+ with N_2 and O_2 is given by

$$O^+ + O_2 \xrightarrow{\beta_1} O_2^+ + O \tag{4}$$

$$O^+ + N_2 \xrightarrow{\beta_2} NO^+ + N \tag{5}$$

In order to study the variations of the electrostatic potential that occur during the first moments of sunrise, for different seasons and near auroral latitudes, the dynamic of ionospheric plasma located at an altitude of about 400 km and consisting essentially of electrons and oxygen ions O^+ is governed by

$$\frac{\partial n^{O^+}}{\partial t} + \frac{\partial}{\partial x}\left(n^{O^+} v^{O^+}\right) = -\beta_1 n^{O^+} n^{O_2} - \beta_2 n^{O^+} n^{N_2} \tag{6}$$

$$\frac{\partial v^{O^+}}{\partial t} + v^{O^+}\frac{\partial v^{O^+}}{\partial x} = -\frac{1}{m^{O^+}n^{O^+}}\frac{\partial P^{O^+}}{\partial x} - \frac{e}{m^{O^+}}\frac{\partial \phi}{\partial x} + \nu^{(O^+,N_2)}\left(v^{N_2} - v^{O^+}\right) + \nu^{(O^+,e)}\left(v^{e} - v^{O^+}\right) + \nu^{(O^+,O_2)}\left(v^{O_2} - v^{O^+}\right) \quad (7)$$

where

$$P^{O^+} = k_B T^{O^+} n^{O^+} \quad (8)$$

stands for the pressure, T and n correspond to temperature and density, respectively.

In F_2 region the strength of the magnetic field is about 10^{-1} G (Cnossen and Richmond 2008), while the electric field is about $\sim 10^3$ stat V/cm (Foster 1983). So, in momentum equations the magnetic force can be neglected compared to the electric force (as the drift velocity corresponds to $\sim 10^3$ cm/s the ratio of the magnetic force to the electric force is about $\sim 1/10$). In addition, the magnetic filed effect is in general neglected when the transport is considered along the magnetic filed lines so $\mathbf{v} \times \mathbf{B}$ is null or electrons are supposed to be conducted along $\mathbf{B}$ (Blelly et al. 2005).

Electron fluid equations are given by

$$\frac{\partial n_e}{\partial t} + \frac{\partial}{\partial x}(n_e v_e) = P \quad (9)$$

where P stands for the source term corresponding to electron production by photoionization. However, in the present model electrons are considered as a neutralizing background. Knowing that all frequencies of ionization by radiations' impact are of $\sim 10^7$ s^{-1} (Schunk and Nagy 2009), it is reasonable to assume $P \sim 0$, no source terms of electrons are present in continuity and momentum equations. Plasma is studied in the time scale corresponding to the inverse of ionic plasma frequency which is $\sim \sqrt{n} \sim 10^5$ s^{-1}, no change in electron density due to photo-ionization during the expansion time scale. However, Coulomb collisions between electrons and ions give rise to momentum transfer considered in momentum balance equation:

$$\frac{\partial v_e}{\partial t} + v_e\frac{\partial v_e}{\partial x} = -\frac{1}{m_e n_e}\frac{\partial P_e}{\partial x} + \frac{e}{m_e}\frac{\partial \phi}{\partial x} + \nu^{(e,O^+)}\left(v^{O^+} - v_e\right) + \nu^{(e,O_2^+)}\left(v^{O_2^+} - v_e\right) + \nu^{(e,N_2^+)}\left(v^{N_2^+} - v_e\right) \quad (10)$$

where

$$P_e = k_B T_e n_e \quad (11)$$

here ϕ and k_B correspond to the plasma electrostatic potential and Boltzmann constant, respectively. $m^{O^+}(m_e)$, $n^{O^+}(n_e)$, $v^{O^+}(v_e)$, $P^{O^+}(P_e)$ and $T^{O^+}(T_e)$ stand for oxygen ion (electron) mass, density, velocity, pressure and temperature, respectively. ν^{jk} are collision frequencies between species j and i. In this work we consider the isothermal expansion case. Isothermal approximation can be used when the plasma is supposed to occupy the half-space at a constant temperature. This is a reasonable assumption due to the huge difference between the expansion time scale (μs) and the temperature changes occurring in one day.

The term $\nu^{(e,k)}(v^{ik} - v_e)$ describes the Coulomb elastic collision between ions and electrons, while the term $\nu^{(O^+,j)}(v^j - v^{O^+})$ describes the interaction with heavy plasma particles.

The collision frequency between electrons and ions is given by (Drellishak et al. 1963)

$$\nu^{(e,i)} = 54.5 \times 10^{-6}\frac{n_i}{T_e^{3/2}} \quad (12)$$

and the one between ions and neutral atoms or molecules corresponds to (Drellishak et al. 1963)

$$\nu^{(i,n)} = 2.6 \times 10^{-15}\frac{m_i n_n}{m_i + n_n}\sqrt{\frac{\alpha e^2(m_i + n_n)}{m_i n_n}} \quad (13)$$

To maintain quasi-neutrality, the system dimensions are assumed to be larger than the Debye length so that we can assume quasi-neutrality with O^+ as a dominant ion species ($\sim 10^6$ cm^{-3}, other ionic species can be neglected compared to this value):

$$n^{O^+} - n_e = 0 \quad (14)$$

At the first moments of the sunrise corresponding to the earlier stage of the expansion, the charge neutrality condition leads to $n_o^{O^+} = n_{eo} = n_o$. As the density of particles in the night-side region is very high, the space scale associated to Poisson's equation becomes very small (Degond et al. 2003). Therefore, the ambipolar electrostatic potential can be found implicitly using the quasi-neutrality assumption.

3 Self-similar solution

In order to get dimensionless equations, time t is normalized by the inverse of ion plasma frequency ω_p and space coordinate x by the Debye length, that is (Fermous and Djebli 2015)

$$X = x/\lambda_{De}, \quad \lambda_{De} = \sqrt{k_B T_e/4\pi n_o e^2}$$
$$T = \omega_p t, \quad \omega_p = \sqrt{4\pi n_o e^2/m^{O^+}} \quad (15)$$

Table 1 Spring data corresponding to march 2016

Day	t_0 (H)	n_e (m^{-3})	n_{O^+} (%)	n_O (cm^{-3})	n_{O_2} (cm^{-3})	n_{N_2} (cm^{-3})	T_i (K)	T_e (K)
1	5.51	0.10986×10^{12}	97.3	3.497×10^7	1.652×10^4	6.546×10^5	1075.0	2162.6
21	5.21	0.1215×10^{12}	97	3.870×10^7	2.328×10^4	9.051×10^5	1084.9	2106.3
30	5.07	0.12451×10^{12}	97	4.014×10^7	2.763×10^4	1.064×10^6	1090.3	1962.3

We then choose the following self-similar variable

$$\xi = X/T = x/c_s\, t, \quad c_s = \sqrt{k_B T_e/m^{O^+}} \tag{16}$$

Densities, velocities, and the electrostatic potential are normalized according to

$$v_j = c_s V_j, \qquad n_j = \frac{n_{jo} N_j}{\omega_p t} \quad \text{and} \quad \phi = \frac{k_B T_e \Phi}{e} \tag{17}$$

where c_s is the ion acoustic velocity and n_{jo} are initial densities. V_j, N_j and Φ are dimensionless parameters.

Using the transformation (16) and the normalization given by (17) the set of partial differential equations (6)–(11) governing the plasma expansion are transformed into ordinary differential equations,

$$\frac{dV^{O^+}}{d\xi} + \frac{1}{N^{O^+}}\left(V^{O^+} - \xi\right)\frac{dN^{O^+}}{d\xi} + \frac{V^{O^+}}{\xi} = 1 - \beta_1' N^{O_2} - \beta_2' N^{N_2} \tag{18}$$

$$\begin{aligned}\left(V^{O^+} - \xi\right)\frac{dV^{O^+}}{d\xi} + \mu_1\left(\frac{1}{N^{O^+}}\frac{dN^{O^+}}{d\xi} + \frac{1}{\xi}\right) &= -\frac{d\Phi}{d\xi} + \alpha_1\gamma_1 N_e\left(V_e - V^{O^+}\right) \\ &+ \alpha_2\Gamma_1\gamma_2 N^{O_2}\left(V^{O_2} - V^{O^+}\right) \\ &+ \alpha_3\Gamma_2\gamma_3 N^{N_2}\left(V^{N_2} - V^{O^+}\right)\end{aligned} \tag{19}$$

$$\begin{aligned}\left(V_e - \xi\right)\frac{dV_e}{d\xi} + \frac{1}{\alpha_1}\left(\frac{1}{N_e}\frac{dN_e}{d\xi} + \frac{1}{\xi}\right) &= \frac{1}{\alpha_1}\frac{d\Phi}{d\xi} + \gamma_4 N^{O^+}\left(V^{O^+} - V_e\right) \\ &+ \gamma_5 N^{O_2^+}\left(V^{O_2^+} - V_e\right) \\ &+ \gamma_6 N^{N_2^+}\left(V^{N_2^+} - V_e\right)\end{aligned} \tag{20}$$

$$\frac{dV_e}{d\xi} + \frac{1}{N_e}\left(V_e - \xi\right)\frac{dN_e}{d\xi} + \frac{V_e}{\xi} = 1 \tag{21}$$

$$\frac{dN_e}{d\xi} = \frac{dN^{O^+}}{d\xi} \tag{22}$$

where

$$\begin{cases}\beta_1' = \beta_1 \frac{n_o^{O_2}}{\omega_p} \\ \beta_2' = \beta_2 \frac{n_o^{N_2}}{\omega_p} \\ k = 54.5 \times 10^{-6}\end{cases} \qquad \begin{cases}\alpha_1 = \frac{m_e}{m^{O^+}} \\ \alpha_2 = \frac{m^{O^+}}{m^{O^+} + m^{O_2}} \\ \alpha_3 = \frac{m^{O^+}}{m^{O^+} + m^{N_2}}\end{cases}$$

$$\begin{cases}\gamma_1 = \frac{k.n_{eo}}{T_e^{3/2}\omega_p} \\ \gamma_2 = \frac{n_o^{O_2}}{\omega_p} \\ \gamma_3 = \frac{n_o^{N_2}}{\omega_p}\end{cases} \quad \text{and} \quad \begin{cases}\gamma_4 = \frac{k.n_o^{O^+}}{T_e^{3/2}\omega_p} \\ \gamma_5 = \frac{k.n_o^{O_2^+}}{T_e^{3/2}\omega_p} \\ \gamma_6 = \frac{k.n_o^{N_2^+}}{T_e^{3/2}\omega_p}\end{cases} \tag{23}$$

$$\mu_1 = \frac{T^{O^+}}{T_e}, \quad \Gamma_1 = 2.6 \times 10^{-15}\sqrt{\frac{\alpha e^2(m^{O^+} + m^{O_2})}{m^{O^+} m^{O_2}}} \quad \text{and} \quad \Gamma_2 = 2.6 \times 10^{-15}\sqrt{\frac{\alpha e^2(m^{O^+} + m^{N_2})}{m^{O^+} m^{N_2}}} \tag{24}$$

4 Results and discussions

The set of ordinary differentials equations (18)–(22) is solved using a numerical Rung-Kutta method with an adequate converging step. The boundary conditions correspond to an equilibrium state for which the plasma starts to expand. As quasi-neutrality is supposed to occur right at the beginning of the expansion, the electric filed is given by $E_o = (4\pi n_o k_B T_e)$ (Mora 2003). So, the initial ambipolar electrostatic potential, at the beginning of the expansion, is $\phi(\xi) = -E_o\xi$, in the numerical code we selected $\xi_o = 0$ so $\phi(\xi = \xi_o) = 0$. Input parameters corresponding to a height of 400 km, latitude of 36.75° and a longitude of 3° are obtained from the International Reference Ionosphere (IRI) model for electrons-ions densities and temperatures. While MSIS model (2012) is used to obtain neutral densities. For example data corresponding to spring season are given by Table 1. The corresponding data for the remaining seasons are implemented to the numerical calculation following the same procedure. Figure 1 shows that there is no big difference between the spring and the summer seasons. For these two seasons, the intensity of the sun radiations is so great to produce plasmas containing

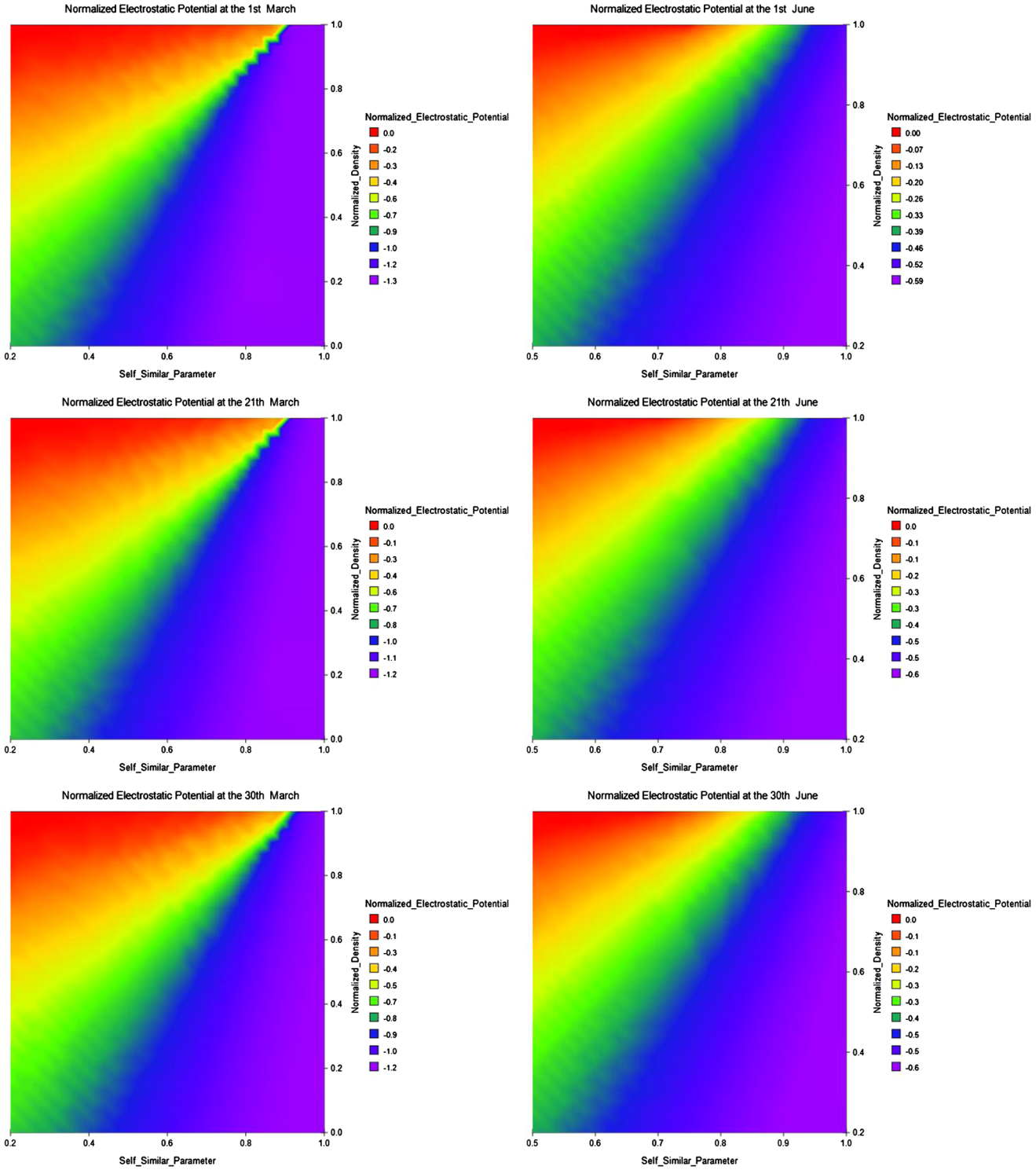

Fig. 1 Electrostatic potential variations using contour plot. Left during March equinox and right during June solstice

ions and energetic electrons. We only considered ionization-recombination processes due to collision between heavy species i.e., ions and neutral particles. Although electron impact is the dominant ionization mechanism in plasma it is not considered in this work because ion-neutral collisions are, the main mechanism of ion's formation in the Earth's ionosphere (Nagy et al. 2009). However, at the earlier stages the potential strength is much important during the hot season. Recombination processes are temperature dependent, when the ion density increases the potential also

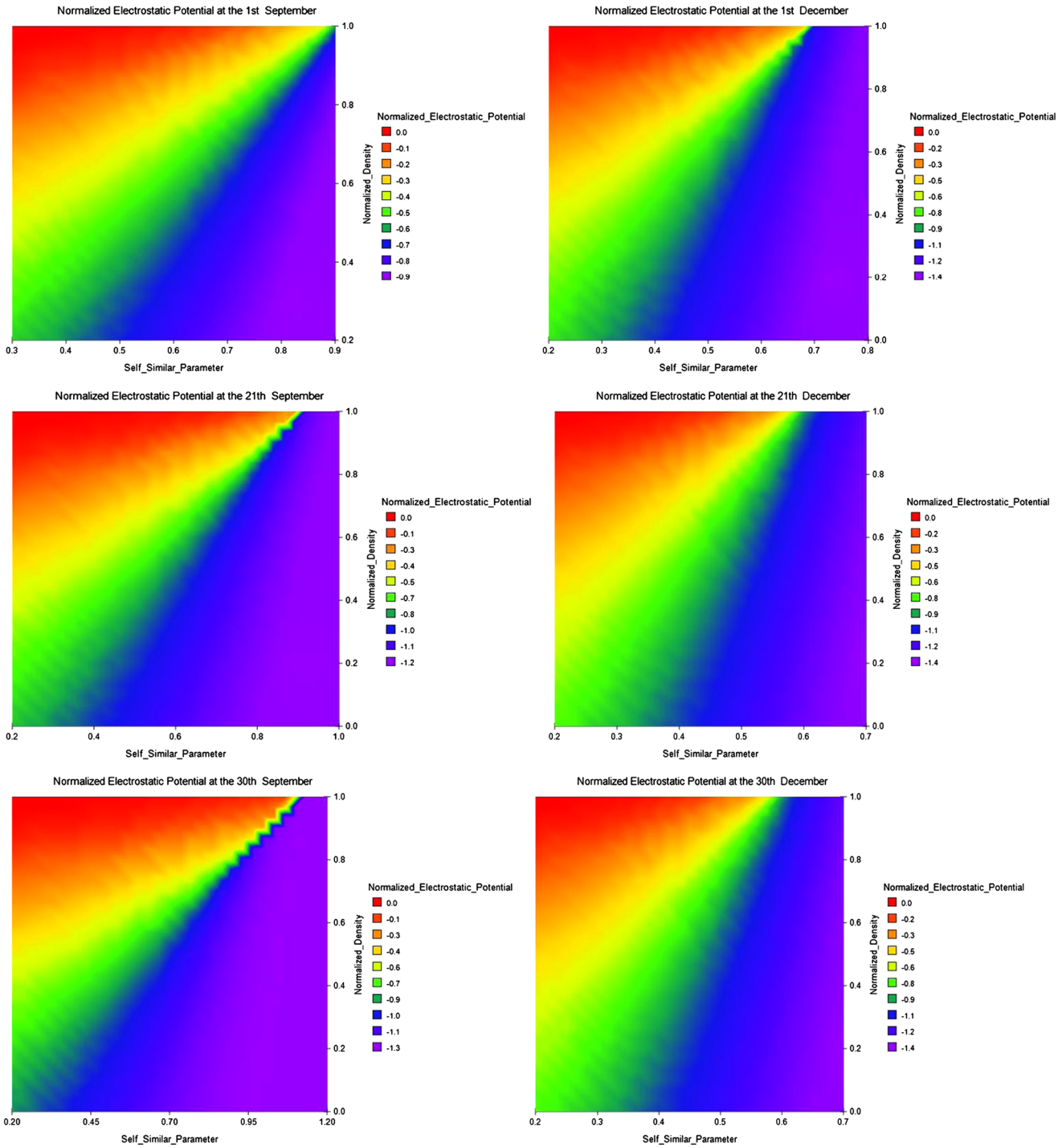

Fig. 2 Electrostatic potential variations. Left during September equinox and right during December solstice

increases. Note also that the potential is negative due to the electron front formed at the head of the expanding plasma. So the negative aspect is a signature of this effect. Later, ions are pulled by the ambipolar electric potential to balance such a local charge separation leading to a positive electrostatic potential. During June these negative values are reached at the earlier stages of the expansion as results of higher electron kinetic energy. It is also worth emphasizing that the instabilities rise during March (less hot than June), and become weaker when days are hotter to vanish when solar intensity is almost similar all days. Thus, we recall previous results that the electric field (potential) depends on the universal time and solar activity (Denisenko et al. 2019).

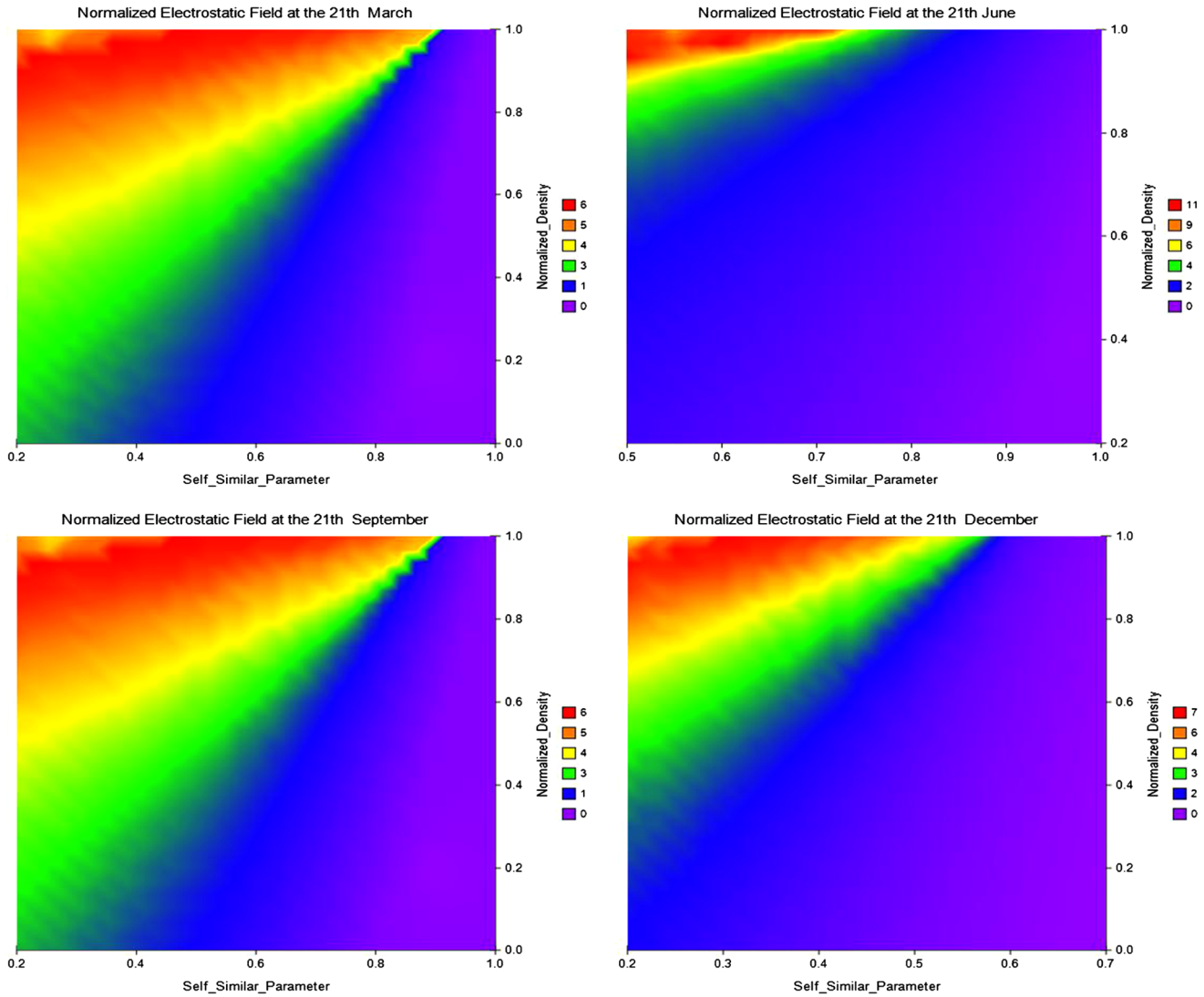

Fig. 3 Comparison of electrostatic field variations during all seasons of 2016

Most important changes can be depicted from Fig. 2 which corresponds to colder seasons. Close to the plasma source region the strength of the electrostatic potential is clearly smaller because of the weak dynamics of all species. The characteristic of the local charge separation length is reduced.

As the electric filed in the F-region can map upward to the magnetosphere and create motions there (Kelley 2014), in Fig. 3 we have gathered the electric field variation during all seasons (obtained by numerical differentiation of the potential). Far away from the plasma production conditions the field strength vanishes, the hotter the month the faster this value is reached. Recombination processes are not significant. Such processes are temperature dependent leading to a low probability for chemical reactions, giving plasma of roughly constant ion densities relay on a constant electrostatic field. Lower temperatures at sunrise are observed in autumn and winter where the plasma density ratios change. Far away from the source, the electrostatic field becomes positive and of lower intensity. This is due to electron low mobility which makes them close to the plasma bulk. Recently, Denisenko et al., by using a mathematical simulation of the ionospheric electric field, have shown that the strength of such a field is about $\sim 10^{-10}$ Stat V/cm. Thus, at present time the electric field could not be detected experimentally (Denisenko et al. 2019). However, our investigation shows that the electric potential is subject to more variations that are in the range -1.7×10^{-4} to -9.7×10^{-4} stat V (-0.05 to -0.29 V), which can be measured as reported by Lee et al. The potential drops are found to be mainly controlled by the cold ionospheric plasmas (Lee et al. 2014). Our investigation shows that most the important potential drop occurs during winter season (December).

5 Conclusion

A qualitative description of the electrostatic potential (field) in the F region of the Earth's ionosphere, where ionic oxygen is the dominant species, is given. To obtain such description, we used the self-similar approach applied to fluid equations governing the dynamics of plasma mix. In this plasma and due to solar activities the collision between heavy species is found to play a crucial role. The negative strength of the electrostatic potential rises at the earlier stages particularly for hotter months, where local charge separation between ions and electrons is more important. The electric field variations are found too small to be measured experimentally while the potential variations are significant showing an important drop during the cold season.

References

Blelly, P.-L., Lathuillère, C., Emery, B., Lilensten, J., Fontanari, J., Alcaydé, D.: Ann. Geophys. **23**, 419 (2005)

Buonsanto, M.J.: Space Sci. Rev. **88**, 563 (1999). https://doi.org/10.1023/a:1005107532631

Chang, T.: Eos Trans. AGU **68**(8), 108 (1987)

Chiu, Y.T., Schulz, M.: J. Geophys. Res. **83**, 629 (1978). https://doi.org/10.1029/ja083ia02p00629

Cnossen, I., Richmond, A.D.: J. Atmos. Sol.-Terr. Phys. **70**, 1512 (2008). https://doi.org/10.1016/j.jastp.2008.05.003

Degond, P., Parzani, C., Vignal, M.H.: Math. Comput. Model. **38**, 1093 (2003). https://doi.org/10.1016/s0895-7177(03)90109-9

Denisenko, V.V.: Russ. J. Phys. Chem. B, Focus Phys. **9**, 789 (2015). https://doi.org/10.1134/s199079311505019x

Denisenko, V., Rycroft, M., Harrison, R.: Surv. Geophys. **40**(1), 1 (2019)

Drellishak, K.S., Knopp, C.F., Cambel, A.B.: Phys. Fluids **6**, 1280 (1963). https://doi.org/10.1063/1.1706896

Fan, Y., Du, X., An, Z., Liu, J., Tan, D., Chen, J.: Acta Geophys. **63**(3), 679 (2015). https://doi.org/10.1515/acgeo-2015-0015

Fermous, R., Djebli, M.: Phys. Plasmas **22**, 042107 (2015). https://doi.org/10.1063/1.4917078

Foster, J.C.: J. Geophys. Res. **88**, 981 (1983). https://doi.org/10.1029/ja088ia02p00981

Gurevich, A.V., Pariĭskaya, L.V., Pitaevskiĭ, L.P.: Sov. Phys. JETP **22**, 449 (1966)

Haider, S.A., Abdu, M.A., Batista, I.S., Sobral, J.H., Xiaoli, L., Esa, K., Maguire, W.C., Verigin, M.I., Singh, V.: J. Geophys. Res. Space Phys. **114**(A3), 03311 (2009). https://doi.org/10.1029/2008JA013709

Hazra, P., Islam, T.: Lect. Notes Electr. Eng. **335**, 185 (2015). https://doi.org/10.1007/978-81-322-2274-3-23

Kelley, M.C.: The Earth's Electric Field: Sources from Sun to Mud. Elsevier, Waltham (2014)

Lee, J., Lee, E., Lee, J., Kim, K.-H., Seon, J., Lee, D.-H., Jin, H., Kim, E.-H., Jeon, H.-J., Lim, S.-B., et al.: J. Astron. Space Sci. **31**(4), 311 (2014)

Makhlouf, S., Djebli, M.: Acta Geophys. **67**, 1671 (2019). https://doi.org/10.1007/s11600-019-00358-3

Markson, R., Price, C.: Atmos. Res. **51**(3–4), 309 (1999)

Mora, P.: Phys. Rev. Lett. **90**, 185002 (2003). https://doi.org/10.1103/physrevlett.90.185002

Nagy, A.F., Balogh, A., Cravens, T.E., Mendillo, M., Mueller-Wodarg, I. (eds.): Comparative Aeronomy, 1st edn. Space Sciences Series of ISSI 29. Springer, New York (2009)

Park, C.G.: J. Geophys. Res. **81**, 168 (1976). https://doi.org/10.1029/ja081i001p00168

Rishbeth, H.: Rev. Geophys. **6**, 33 (1968). https://doi.org/10.1029/rg006i001p00033

Rishbeth, H., Garriott, O.K.: Introduction to Ionospheric Physics. International Geophysics, vol. 14. Academic Press, New York (1969)

Rycroft, M.J., Odzimek, A.: In: 2011 XXXth URSI General Assembly and Scientific Symposium. IEEE, New York (2011). https://doi.org/10.1109/ursigass.2011.6050943

Ryu, K., Chae, J.-S., Lee, E., Parrot, M.: J. Atmos. Sol.-Terr. Phys. **121**, 110 (2014). https://doi.org/10.1016/j.jastp.2014.10.003

Samir, U., Wright, K.H., Stone, N.H.: Rev. Geophys. **21**, 1631 (1983). https://doi.org/10.1029/rg021i007p01631

Schunk, R., Nagy, A.: Ionospheres: Physics, Plasma Physics, and Chemistry, 2nd edn. Cambridge Atmospheric and Space Science Series. CUP, Cambridge (2009)

Schunk, R.W., Szuszczewicz, E.P.: J. Geophys. Res. **96**, 1337 (1991). https://doi.org/10.1029/90ja02345

Singh, N., Schunk, W.: J. Geophys. Res. Space Phys. **87**, 9154 (1982). https://doi.org/10.1029/ja087ia11p09154

Stening, R.J.: Planet. Space Sci. **21**, 1897 (1973). https://doi.org/10.1016/0032-0633(73)90119-0

Watanabe, S., Oyama, K.I., Abdu, M.A.: J. Geophys. Res. **100**, 14581 (1995). https://doi.org/10.1029/95ja01356

Zhang, X., Zhao, S., Song, R., Zhai, D.: Adv. Space Res. **63**(11), 3536 (2019). https://doi.org/10.1016/j.asr.2019.02.008